Application of ANFIS and GRA for multi-objective optimization of optimal wire-EDM parameters while machining Ti–6Al–4V alloy

Sandeep Kumar[1] · S. Dhanabalan[2] · C. S. Narayanan[3]

Abstract

The applications of artificial intelligence (AI) mainly, the hybrid approaches are becoming more popular and the relevant researches have been conducted in every field of engineering and science by using these AI techniques. Therefore, this research aims to examine the influence of wire electric-discharge machining parameters on performance parameters to improve the productivity with a higher surface finish of Titanium alloy (Ti–6Al–4V) by using the artificial intelligent technique. In this experimental analysis, the adaptive network based fuzzy inference system (ANFIS) model has been highly-developed and the multi-parametric optimization has been done to find the optimal solution for the machining of titanium superalloy. The peak current (I_p), taper angle, pulse on time (T_{on}), pulse of time (T_{off}) and the dielectric fluid flow rate had selected as operation constraints to conduct experimental trials. The surface roughness and MRR were considered as output responses. The influence on machining performance has been analyzed by the ANFIS model and the developed model was validated with the full factorial regression models. The developed models showed the minimum mean percentage error and the optimized parameters by the GRA method showed the considerable improvement in the process.

Keywords Wire-EDM · Titanium alloy · GRA · Artificial intelligence techniques · ANFIS

1 Introduction

Non-conventional machining processes are the requirements of the fastest growing industries because of the precision, complex, intricate shape of the work material, higher tolerances and economically. Hard materials and super alloys such as titanium alloys, tungsten carbides, high carbon tool steels generally used in tool industries, automotive and electronics industries, medical and aerospace are very difficult—to-machine by conventional manufacturing processes. Therefore, the ease of material cutting and machining non-conventional machining is preferred. WEDM is generally used to produce complex shapes die cavities and forming tools, fixtures, gauges, etc. which are difficult to produce by means of any other conventional and non-conventional machining methods except micro-machining [1].

Titanium alloys (Ti-alloys) are mostly utilized in aerospace and automotive industries to manufacture higher precision components. Ti–6Al–4V grade 5 titanium alloy is used for the manufacturing of diesel engine components such as connecting rods, gas turbine parts, intake valves, etc. and this alloy covers the 50% of total global consumption [2].

WEDM is a variation and development of EDM. In 1969, the Swiss firm Agie developed and delivered the world's initially WEDM machine. These machines had machining ability to cut the material about 21 mm^2/min per hour. These machines were extremely slow in production rate. After the continuous improvements in the machining

ability, the machining speed improved. WEDM removes material from the work metal with the use of electricity by means of spark erosion as shown in Fig. 1 [1, 3]. It is most important requirement that the work material should be electrically conductive. AC servo motors are exploited to provide positioning, stability and enhancement of wire tension. A DC or AC servo mechanism maintains the gap (0.051–0.076 mm) between the electrode and the work material. This maintained gap prevents the short circuiting of wire.

'Dielectric' is the shield between the wire electrode and material. De-ionized water is generally used as a dielectric medium because the dielectric medium acts as an insulator. In this process, the material is submerged in the dielectric medium. When the voltage is applied, the electric pulses are generated, fluid ionizes and a spark generates between the electrode wire and work material, the controlled spark precisely erodes the metal from the work material causing it to melt and vaporize. Pressurized dielectric fluid flows continuously. It cools the vaporize material and carry away the particles from the cutting section. The dielectric passes through the filter to remove suspended particles and it is used continuously. Chillers are used to maintain the temperature of dielectric fluids for higher machining efficiency and accuracy. In WEDM the wire electrode never comes in contact with the work piece, therefore this process is stress free cutting operation [1, 4–6].

Various researchers have been reported working on WEDM to measure the influence of input parameters on performance parameters such as, Liao and Woo [7] reported the influence of wire-EDM constraints such as 'on time' (T_{on}), 'off time' (T_{off}) and feed rate on the behavior of pulse train i.e. short ratio, arc ratio, normal ratio and gap width. Experiments were conducted on SKD 11 tool steel. The authors concluded that 'on time' was a significant factor for arc ratio [7]. Miller et al. [6] demonstrated the capability of WEDM to machine advanced

materials such as porous metal foams, diamond grinding wheels, sintered Nd–Fe–B magnets, etc. Author examined the influence of spark on time duration and spark on time ratio on surface roughness and MRR by using Brother HS-5100 WEDM [6].

Mahapatra et al. [8] optimized the WEDM performance parameters such as MRR, SR and kerf width by using the Taguchi method. ROBOFIL100 5-axis CNC WEDM was used for experimental work. Experiments were conducted on D2 tool steel by using zinc-coated copper wire having 0.25 mm diameter. The author concluded that discharge current, pulse duration and the dielectric flow rate had the significant effect on the performance parameters.

Kumar et al. [9] demonstrated the effect of T_{on} (pulse on time), T_{off} (pulse off time), I_p (peak current), spark gap voltage, wire feed (WF) and wire tension (WT) on the surface roughness of machined titanium grade-2 workpieces. The author concluded that pulse on time, pulse off time, peak current and spark voltage had higher impact on surface roughness [9]. Manjaia et al. [10] statistically optimized the pulse on time, pulse off time, servo voltage and wire feed for WEDM of AISI D2 tool steel for the response of MRR and SR. The author resulted the higher significance of pulse on time and servo voltage on performance parameters [10].

Kumar et al. [11] concluded that the surface roughness increases with the increase in peak current because peak current increases the discharge energy. They conducted the experimental work on tungsten carbide with brass wire. Wire feed, flushing pressure and current were the significant parameters for surface roughness [11]. Vijaya Babu [12] concluded that the peak current was the significant parameter for surface roughness after they studied the effect of pulse on time, pulse off time and peak current on Inconel 625. Maniappan et al. [13] reported the influence of peak current on kerf width. The experiments were conducted on Al 6061 alloy with zinc coated brass wire [13].

Various researchers have been reported the use of ANFIS to predict the performance of machining such as turning, ball milling, WEDM etc. Kar et al. [14] explained the applications of Neuro-fuzzy system in various fields such as stock market, financial trading, hazard assessment, etc. Caydas et al. [15] worked to measure the impact of pulse duration, open circuit voltage, wire feed and dielectric flushing pressure on white layer thickness and SR. Author developed the ANFIS model for the prediction of performance parameters [15].

Hossain and Ahmad [16] developed the ANFIS model for the prediction of performance parameters of ball end milling. The authors compared the ANFIS model results with the response surface methodology and found more accurate [16]. Abdul Mayu et al. developed the ANFIS model for the prediction of hardness of TiAlN coatings. Author compared and validated their model with fuzzy
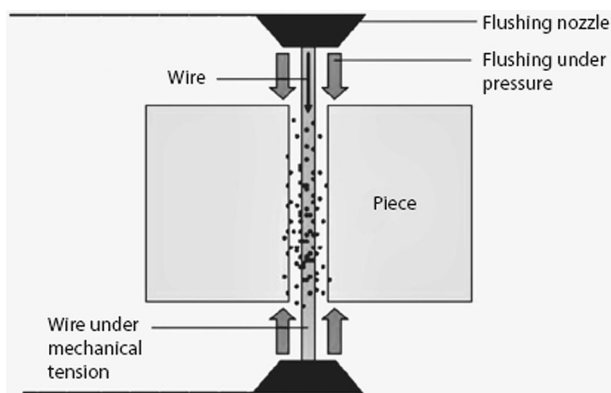

Fig. 1 Working principle of WEDM

and RMS model. They concluded that the triangular membership function obtains best results than other MF's.

Anwar et al. [5] demonstrated the ANFIS model for the prediction of surface roughness and chipping size of rotary ultrasonic drilling (RUM). The authors compared the ANFIS results with the regression models. They achieved the lover mean absolute percentage error in ANFIS model [5].

Boral and Chakraborty [17] developed case-base reasoning system for machine tool selection and for non-traditional machining process selection. Sarikaya et al. developed a multi-objective optimization model for the selection of micro-electrical discharge drilling of AISI 304 stainless steel using S/N, RSM, RA and ANN method [18–20]. Chatterjee et al. proposed a novel hybrid model encompassing factor relationship (FARE) and MABAC (multi-attributed border approximation area comparison) method for selection and evaluation of non-conventional machining [21, 22].

From the literature survey, it is ascertained that no plausible work has been reported on the application of ANFIS system in WEDM. Therefore, the main objective of this work is, (1) to optimize the performance parameters by multi-parametric optimization using grey relation method (GRA) and (2) to develop the ANFIS model for the prediction of two major performance parameters namely surface roughness and material removal rate in WEDM by considering the five major input parameters.

2 Methodology

Design-of-experiments (DOE) needs cautions scheduling, practical layout of trials, Taguchi method has identical procedures for every DOE application steps and DOE can dramatically decrease the amount of trials [4, 18]. Thus, the five parameters such as Taper angle (U and V axis taper in degrees), pulse on time (T_{on}), peak current (I_p), dielectric flow rate and pulse off time (T_{off}) had selected for the governing parameters. Each parameter had three levels denoted by level-1, level-2 and level-3 except taper angle. Taper angle had two levels. From the previous literatures, it is clear that the taper angle has the least influence on performance parameters. Therefore, the taper angle has selected two levels to reduce the number of experimental trials and mixed orthogonal array is used, as designated in the Table 1.

2.1 Experimental set-up

As per DOE, the experiments were performed on ELEKTRA Ultima-1F WEDM. The WEDM setup is shown in Fig. 2.

Titanium alloy namely Ti–6Al–4V grade-5 superalloy was used in the form of thick rectangular plate.

Table 1 Allocated values of WEDM constraints and their levels

Factor	Parameter	Units	Level-1	Level-2	Level-3
A	Taper Angle	Degree	3	1.5	–
B	Peak Current (I_p)	Amps	110	120	130
C	Pulse on Time (T_{on})	µs	104	108	112
D	Pulse off time (T_{off})	µs	55	58	63
E	Dielectric flow rate	Ltr/min	10	12	15

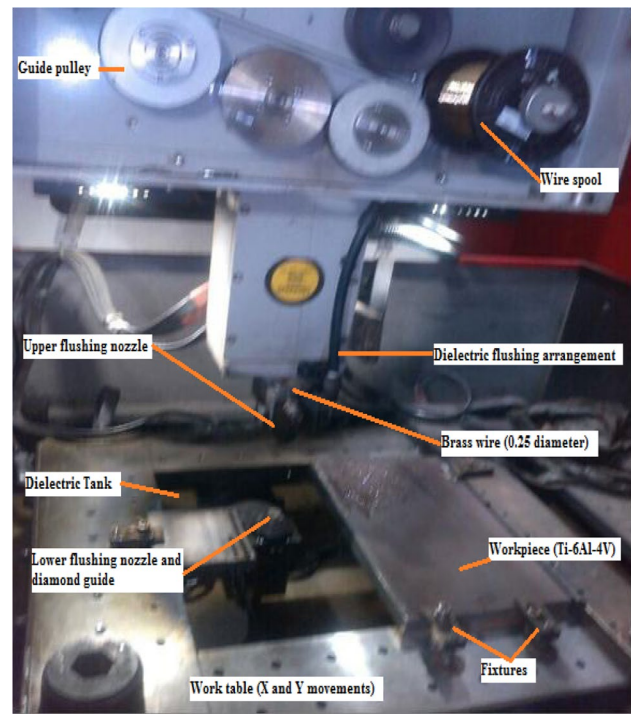**Fig. 2** Experimental setup of ELEKTRA Ultima-1F WEDM

Ti–6Al–4V material belongs to (α + β) category of titanium alloys and its chemical composition consists of 5.5–6.5% Al, 3.5–4.5% V, 0.08% C, 0.005% Yttrium, 0.30% Fe and remaining titanium. This superalloy has excellent mechanical properties, acceptable fracture toughness, high strength and resistance to corrosion. Therefore, this superalloy is mostly demanded in aerospace, chemical, heat treatment, nuclear and gas turbine industries. The workpiece and the zinc coated brass wire electrode having diameter 0.25 mm was linked up with +ve and −ve polarity in the D.C. power source, respectively. De-ionized water having a conductivity level of 0.6 µs/cm was used as dielectric medium. The dielectric fluid was flushed from the top and bottom nozzles.

Surface roughness of the machined samples was measured with Mitutoyo surf-test surface roughness tester. Each sample was evaluated thrice and the mean

values were obtained. The mathematical relation used to evaluate the surface roughness is given in Eq. 1.

$$Surface\ roughness\ (Ra) = \frac{1}{L} \int_0^L |Zx| \langle dx \rangle \quad (\mu m) \qquad (1)$$

where Ra is the value of surface roughness measured in µm, L = evaluation length and Z(x) = profile height function.

The ANOVA mathematical relation (lower the better) applied to calculate the S/N ratio of SR is given in Eq. 2

$$\eta_{HB} = -10 \log \left[\frac{1}{n} \sum_{i=1}^{n} y_i \right] \qquad (2)$$

The ANOVA mathematical relation (higher the better) used to calculate the S/N ratio of MRR is given in Eq. 3

$$\eta_{HB} = -10 \log \left[\frac{1}{n} \sum_{i=1}^{n} y_i \right] \qquad (3)$$

The S/N ratio (n_{ij}) for the ith performance characteristics in the jth experiment is evaluated by the Eq. 4.

$$\eta_{ij} = -10 \log[L_{ij}] \qquad (4)$$

The mathematical relation used to evaluate the material removal rate (MRR) is given in Eq. 5.

$$MRR = \frac{Weight\ of\ work\ material\ removal}{time} \quad (g/min) \quad (5)$$

3 ANFIS modeling for performance prediction

The growing need of artificial intelligence (AI) system to solve out the complex and real world problems, the ANN and fuzzy interference system has drawn the concern of researchers in engineering and various scientific areas. In 1983, Jang proposed a Neuro-fuzzy system (NFS) which is the combination of ANN (artificial neural network) and Fuzzy-logic [23]. This system combines the reasoning of fuzzy system with the structure of neural networks. This system provides the flexible approximation with the ability to explore interpretable If–then fuzzy rules. ANFIS uses a hybrid learning method to determine the optimum distribution of various MF's (membership functions) and provides the mapping relations between input and output data. ANFIS uses the combined architecture of ANN and Fuzzy-logic [23]. In ANFIS the MF's function parameters are updated by two approaches, namely hybrid and back propagation. The architecture of ANFIS consists of 5 layers and each layer of the ANFIS architecture is described by node function. The co-operative Neuro
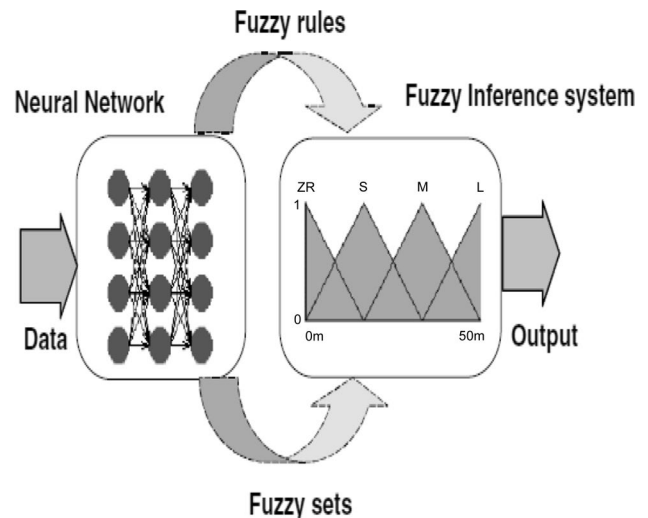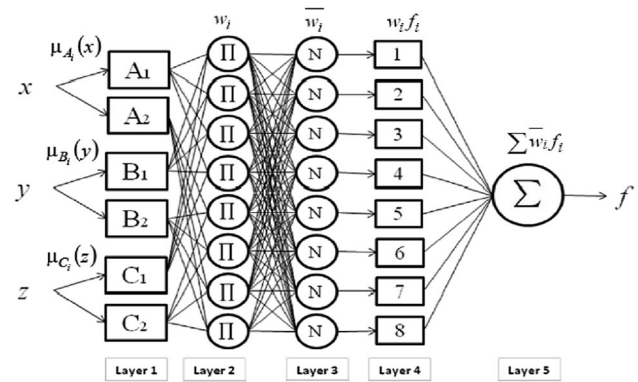

Fig. 3 Co-operative neuro fuzzy model

Fig. 4 ANFIS architecture

fuzzy model is shown in the Fig. 3 and the architecture of ANFIS system with layers and nodes is shown in Fig. 4.

The ANFIS uses the Takagi–Sugeno type fuzzy If–then rules and the five network layers are used to perform the fuzzy interference steps. The steps used in ANFIS are described as:

- Calculation of the MF's values (Fuzzyfication): In the ANFIS architecture μA_i, μB_i, and μC_i are the MF's of three input values x, y and z respectively and each node produces the MF's of input values. The Eq. 6 describes the MF's for bell shaped function:

$$\mu A_i(x) = \frac{1}{1 + \left[\left(\frac{x - c_i}{a_i} \right)^2 \right] \times b_i} \qquad (6)$$

where a_i, b_i and c_i—parameter set and these set changes the FMS form in between 0 and 1 value.

- Multiplication of the incoming signals by applying Fuzzy operator (Eq. 7)

$$i = \mu A_i(x) \times \mu B_i(y) \times \mu C_i(z) \qquad (7)$$

where $i = 1, 2 \ldots$.

- Normalization of node firing strength: The normalization of the firing strength of each node is calculated by the Eq. 8

$$\overline{w}_i = \frac{w_i}{\sum_i w_i}, \quad i = 1, 2, 3 \ldots \qquad (8)$$

- Defuzzification: Defuzzification is used to convert the fuzzy quantity to predict the accurate value. Each node in the layer 4 in an adaptive node having a node function. The node functions are identified during the network training. In Defuzzification, the MF's and the rules are united and thus providing the results.

$$\overline{w}_i \times f_i = \overline{w}_i \cdot (p_i \cdot x + q_i \cdot y + r_i \cdot z + s_i) \qquad (9)$$

where $p_i, q_i, r_{i=}$ consequent parameter set of each node.

- The summation of all incoming signals: the total of incoming signals is calculated by the relation given in Eq.

$$Output = \sum_i \overline{w}_i \cdot f_i = \frac{\sum_i \overline{w}_i \cdot f_i}{\sum_i \overline{w}_i} \qquad (10)$$

3.1 Results of ANFIS model

The ANFIS model has been developed as the function of WEDM parameters for Ti–6Al–4V titanium alloy by using the eighteen testing data and training data. The already existed algorithm in MATLAB was used to achieve the perfect training and prediction of data. The following Table 2 represents the initial parameters for ANFIS model.

In this ANFIS structure, the hybrid algorithm was used. ANFIS model has the different shape of input and output MF's. From all the MF's the 'trimf' MF's has selected because the trimf MF's (triangular membership functions) has incline and decline features with one certain value and it displays the lowest test error and the lesser value of mean absolute percentage error rather than other MF's [5, 24].

The training was executed using 300 epochs for surface roughness and MRR model. Training curve obtained after data training is shown in Fig. 5.
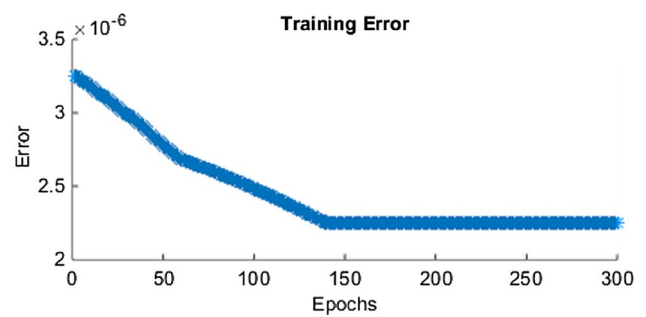

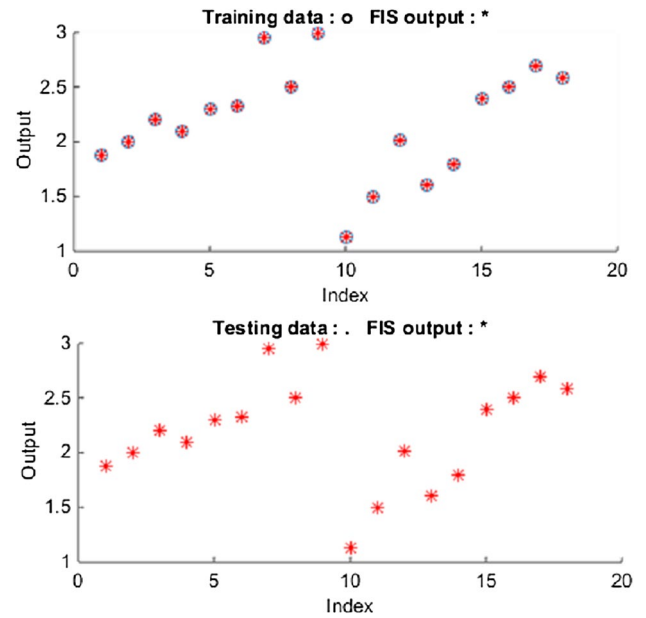**Fig. 5** Training curve for surface roughness model

Fig. 6 Comparison between the experimental and predicted surface roughness by ANFIS test data

The curve was obtained after training the data. The obtained values of training error was 2.2428 * 10⁻⁶. It shows that after 138 epochs, root mean square error become steady because of the limited experimental data. For the prediction of output values for SR, the set of fuzzy interference parameters were chosen in the training phase. The predicted values obtained through the ANFIS model were compared with the experimental values. The comparison between the experimental and predicted surface roughness by ANFIS test data is shown in Fig. 6.

Table 2 Initial parameters for the ANFIS model	Output response	Surface roughness (SR)	Material removal rate (MRR)
	Method of training	Hybrid	Hybrid
	MF's (membership functions)	trimf	trimf
	No. of Mf's	2 3 3 3 3	2 3 3 3 3
	No. of Epochs	300	300
	Output function	Constant	Constant
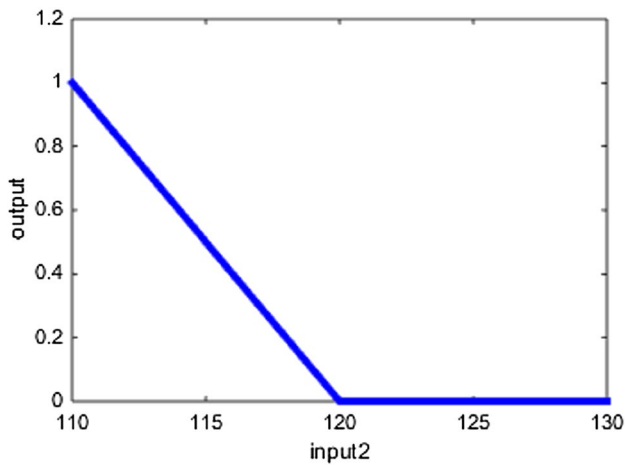
Fig. 7 Influence of peak current (Input2) on surface roughness

Fig. 9 Surface view (Input2-peak current, Input5-dielectric flow rate and output-surface roughness)

Fig. 8 Influence of dielectric flow rate (Input5) on surface roughness

Fig. 10 Training curve for MRR model

The generated model was used to measure the influence of input parameters on the performance parameters namely surface roughness and MRR. Figure 7 demonstrates the influence of peak current on surface roughness. The values of SR was higher initially at the low value of peak current (i.e. 110 amperes) but as the value of peak current increased, the value of surface roughness declined and become constant.

Figure 8 expresses the influence of dielectric pressure on surface roughness. It clearly shows that the value of SR increased with the increase in dielectric flow rate.

Figure 9 demonstrates the surface view for measurement the surface roughness of titanium alloy (Ti–6Al–4V) in relation to change of peak current and dielectric pressure. It shows that the value of SR is higher at 12 Lit/min of dielectric flow rate and 120 amps of peak current. As the value of input constraints had changed, the value
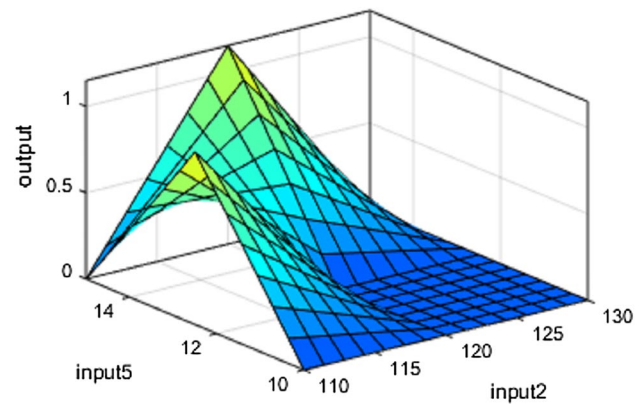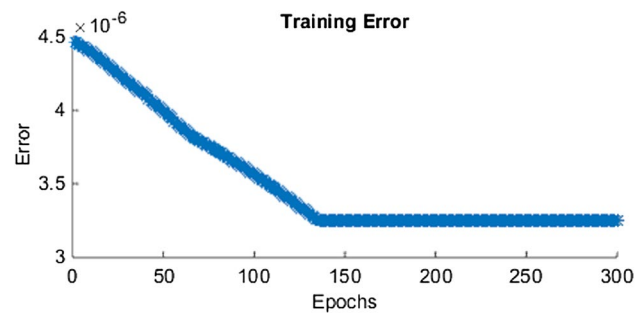
of output responses also varied. The same procedure was used to develop the model for material removal rate (MRR). For the prediction of output values of MRR, the set of fuzzy interference parameters were chosen in training phase. The predicted values obtained through the ANFIS model were compared with the experimental values. The training curve obtained during the MRR is shown in Fig. 10.

The comparison between the experimental and predicted material removal rate (MRR) by ANFIS test data is shown in Fig. 11.

The triangular membership function (Trimf) generated for Input and output variables through ANFIS are shown in Fig. 12.

3.2 Regression analysis and empirical model

In regression equations, the coefficients of determination, R^2 are used to decide whether regression model is appropriate or not. The value of R^2 provides an exact model if the value is 1. In this experimental study, the value of R^2 for SR and MRR is very close to unity. Therefore, this model
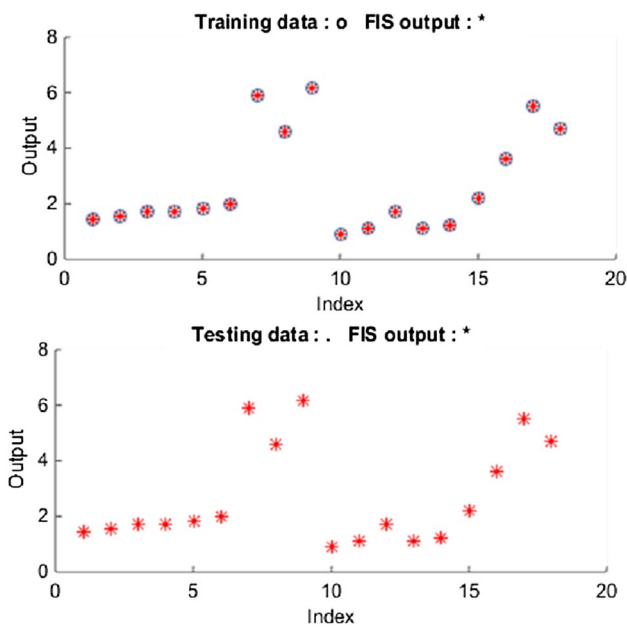
Fig. 11 Comparison between the predicted and experimental MRR by ANFIS test data

is reliable. The calculated regression empirical models for MRR and SR are given in Eqs. 11 and 12.

$$SR = -13.0 + 0.224\,\text{taper angle} + 0.0459\,\text{peak current}$$
$$+ 0.0975\,\text{pulse on time} - 0.0245\,\text{pulse off time}$$
$$- 0.0053\,\text{dielectric flow rate} \tag{11}$$

$$MRR = -33.7 + 0.358\,\text{taper angle} + 0.184\,\text{peak current}$$
$$+ 0.165\,\text{pulse on time} - 0.0871\,\text{pulse off time}$$
$$+ 0.038\,\text{dielectric flow rate} \tag{12}$$

3.3 Comparison of ANFIS model to regression empirical model

The regression equations were obtained by using the full factorial design in Minitab and a comparison between the ANFIS model and Regression model was made to understand the potential of ANFIS. Figure 13 shows the comparison between the regression and ANFIS model.
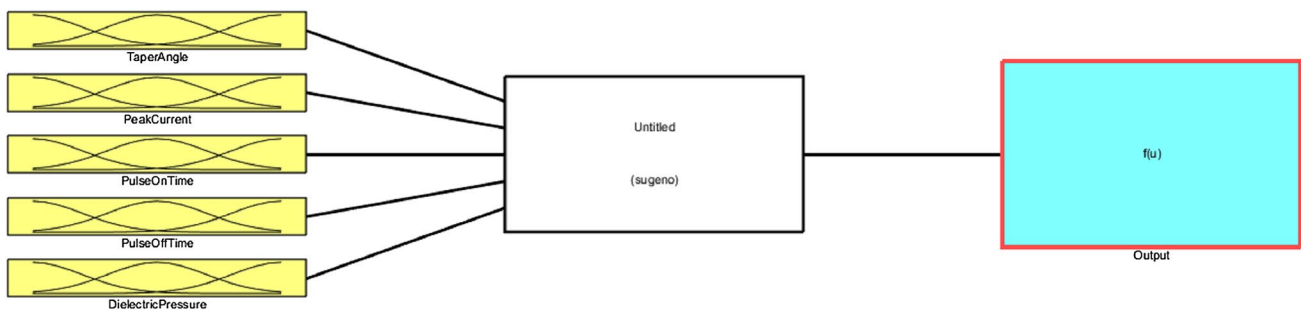

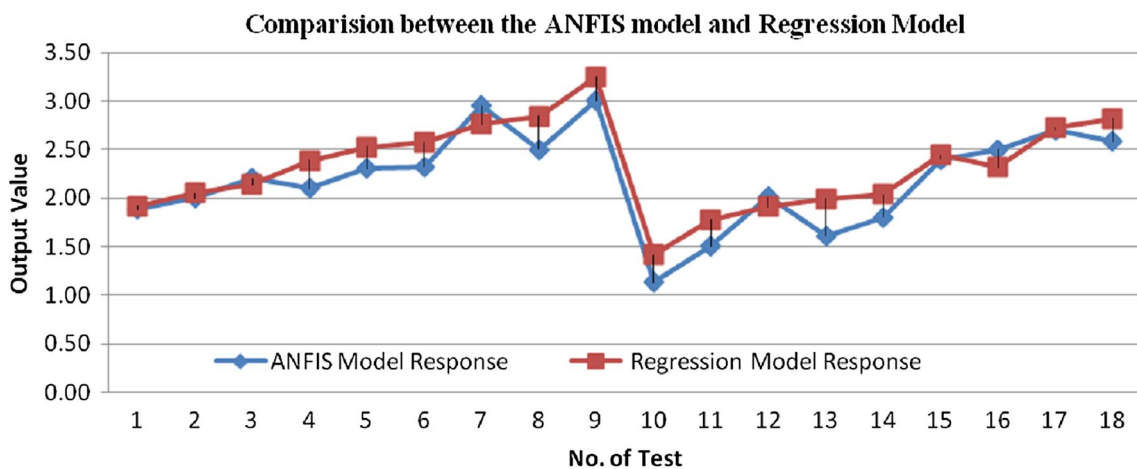**Fig. 12** Trimf MF's for input and output variables (fuzzy-logic designer)

Fig. 13 Comparison between the experimental and predicted MRR by ANFIS test data

From the comparison between the ANFIS model and Regression model responses, it is found that the ANFIS model has a lower value of absolute mean percentage of error than regression model. Therefore, the ANFIS model performance is higher than regression model.

4 DOE and multi-parametric optimization

The aim of multi-parametric optimization is to increase the material removal rate and to minimize the value of surface roughness. In this experimental analysis, L_{18} $(2^1\,3^4)$ mixed orthogonal array (OA) was selected. This OA has 18 parametric combinations; therefore, the total numbers of 18 experiments were conducted to measure the interactions between the various factors. The parameter combinations obtained using the L_{18} $(2^1\,3^4)$ mixed orthogonal array (OA) are shown in Table 3.

4.1 Multi-parametric optimization using the GRA

The steps used for multi-parametric optimization using the grey relational analysis (GRA) are discussed as:

• Normalization of all the experimental results of SR and MRR: Linear normalization of experimental values is performed in the range of 0 and 1. The normalized val-

ues for output responses were calculated by using the standard formula given in Eq. 13.

$$Normalized\ results\ (X_{ij}) = \frac{(y_{ij}) - (min_j\, y_{ij})}{(max_j\, y_{ij}) - (min_{ij}\, y_{ij})} \quad (13)$$

where $y_{ij} =$ ith experiment results in jth experiment.

• Calculation for the Grey relational coefficients: The standard formula used for the computation of Gray relational coefficients is given in Eq. 14.

$$\delta_{ij} = \frac{min_i\, min_j\, \left| x_i^0 - x_{ij} \right| + \xi\, max_i\, max_j\, \left| x_i^0 - x_{ij} \right|}{\left| x_i^0 - x_{ij} \right| + \xi\, max_i\, max_j\, \left| x_i^0 - x_{ij} \right|}, \quad (14)$$
$$0 < \xi < 1$$

where $x_i^0 =$ ideal normalized value.

• Calculation for the Grey relational grade: Grey relational grades are evaluated by the average of Grey relational coefficients using the formula given in Eq. 15. The calculated values for normalization, Grey relational coefficients and grades are shown in Table 4.

$$\alpha_j = \frac{1}{m} \sum_{i=1}^{m} \delta_{ij} \quad (15)$$

Table 3 DOE matrix of L_{18} mixed orthogonal array (OA) and measured values for output responses

Sr. no.	Taper angle (A)	I_p (B)	T_{on} (C)	T_{off} (D)	Dielectric flow rate (E)	Output responses	
						Surface roughness	MRR
1.	3	110	104	55	10	1.88	1.42
2.	3	110	108	58	12	1.98	1.55
3.	3	110	112	63	15	2.16	1.72
4.	3	120	104	55	12	2.07	1.7
5.	3	120	108	58	15	2.24	1.83
6.	3	120	112	63	10	2.32	1.95
7.	3	130	104	58	10	2.95	5.89
8.	3	130	108	63	12	2.5	4.55
9.	3	130	112	55	15	2.99	6.16
10.	1.5	110	104	63	15	1.13	0.8
11.	1.5	110	108	55	10	1.48	1.04
12.	1.5	110	112	58	12	2.01	1.71
13.	1.5	120	104	58	15	1.57	1.07
14.	1.5	120	108	63	10	1.8	1.16
15.	1.5	120	112	55	12	2.38	2.23
16.	1.5	130	104	63	12	2.47	3.58
17.	1.5	130	108	55	15	2.67	5.52
18.	1.5	130	112	58	10	2.58	4.69

Table 4 Calculated values for grey relational grades

Sr. no.	S/N ratio		Normalization		Deviation sequence		Grey relational coefficients		Grades
	Surface roughness	MRR	Surface roughness	MRR	Surface roughness	MRR	Surface roughness	MRR	
1.	− 5.483	3.046	0.52136	0.23629	0.47864	0.76371	0.48954	0.67908	0.58431
2.	− 6.021	3.807	0.58473	0.28168	0.41527	0.71832	0.46094	0.63965	0.5503
3.	− 6.848	4.711	0.68235	0.3356	0.31765	0.6644	0.42289	0.59837	0.51063
4.	− 6.444	4.558	0.6347	0.32649	0.3653	0.67351	0.44064	0.60497	0.52281
5.	− 7.235	5.249	0.72787	0.36773	0.27213	0.63227	0.40721	0.57622	0.49171
6.	− 7.310	6.021	0.73674	0.41375	0.26326	0.58625	0.40429	0.54719	0.47574
7.	− 9.396	15.417	0.98279	0.9743	0.01721	0.0257	0.3372	0.33914	0.33817
8.	− 7.959	13.255	0.81327	0.84533	0.18673	0.15467	0.38073	0.37166	0.37619
9.	− 9.542	15.848	1	1	0	0	0.33333	0.33333	0.33333
10.	− 1.062	− 0.915	0	0	1	1	1	1	1
11.	− 3.522	0.828	0.2901	0.10398	0.7099	0.89602	0.63284	0.82784	0.73034
12.	− 6.064	4.711	0.58984	0.3356	0.41016	0.6644	0.45878	0.59837	0.52858
13.	− 4.137	0.828	0.36258	0.10398	0.63742	0.89602	0.57966	0.82784	0.70375
14.	− 5.105	1.584	0.47682	0.14907	0.52318	0.85093	0.51186	0.77034	0.6411
15.	− 7.604	6.966	0.77146	0.47016	0.22854	0.52984	0.39325	0.51538	0.45431
16.	− 7.959	11.126	0.81327	0.71832	0.18673	0.28168	0.38073	0.4104	0.39556
17.	− 8.627	14.855	0.89209	0.94074	0.10791	0.05926	0.35917	0.34704	0.35311
18.	− 8.232	13.442	0.84553	0.85648	0.15447	0.14352	0.3716	0.3686	0.3701

Table 5 Grey relational grade response table

Factor	Parameter	Level-1	Level-2	Level-3
A	Taper angle	0.4648	0.57521	—
B	Peak current (I_p)	0.65069	0.54824	0.36108
C	Pulse on time (T_{on})	0.59077	0.52379	0.44545
D	Pulse off time (T_{off})	0.49637	0.4971	0.56654
E	Dielectric flow rate	0.52329	0.47129	0.56542

Average grey relational grade = 0.52

Table 6 Confirmation of experiment

Predicted value		Experimentation
Level	$A_2B_1C_1D_3E_3$	$A_2B_1C_2D_1E_1$
SR (µm)	1.48	1.13
MRR (g/min)	1.04	0.8
Grade	0.73034	1
Improvement in grey relational grade: 0.2697		

where α_j = Grey relational grade and m = No. of execution grade characteristics.

- Calculation of the optimum levels: optimum levels are calculated to find the significant parameters as shown in Table 5.
- Selection of the optimum levels of process constraints by taking the highest values of levels for each parameter from the grey response table. The response table is clearly indicating the level values for each process parameter at their different levels. The highest value of the different level shows the best optimized value.
- Confirmation of experiment and verification of the optimized process parameters.

4.2 Confirmation of experiment

After obtaining the optimized values of process parameters, the last step is to confirm the experimentation as shown in Table 6. The mathematical relation used to calculate the estimated grade relational grade is given in Eq. 9.

$$\hat{\alpha} = \alpha_m + \sum_{i=1}^{q} \left(\overline{\alpha}_i - \alpha_m \right) \tag{16}$$

where α_m = total mean of the Grey relational grade at optimum level and q = no. of process parameters.

Taguchi analysis

Taguchi analysis is used for the selection of best optimized parameter value for the individual process parameter and to measure the influence of each parameter at different levels.

4.3 Influence of input constraints on Ra value (SR)

The main effect plot for data means as shown in Fig. 14 is showing the effect of individual parameter at different
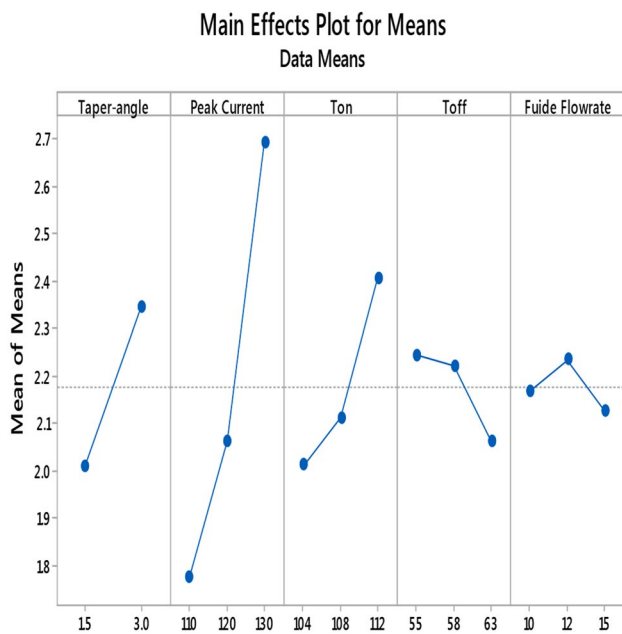
Fig. 14 Main effect plot for data means—SR-(smaller is better)

Fig. 15 Main effect plot for data means—MRR-(larger is better)

Table 7 Response table for means (SR)

Level	Taper angle	Peak current	T_{on}	T_{off}	Dielectric flow rate
1	2.026	1.787	2.028	2.263	2.172
2	2.361	2.088	2.133	2.242	2.252
3	–	2.705	2.418	2.075	2.157
Delta	0.336	0.918	0.390	0.188	0.095
Rank	3	1	2	4	5

Table 8 Levels of selected input parameters at minimum SR

Factor	Taper angle	Peak current	T_{on}	T_{off}	Dielectric flow rate
Level	2	1	1	1	3
Rank	3	1	2	4	5

Table 9 Levels of selected input parameters at maximum MRR

Factor	Taper angle	Peak current	T_{on}	T_{off}	Dielectric flow rate
Level	1	3	3	1	3
Rank	4	1	3	2	5

Table 10 Response table for means (MRR)

Level	Taper angle	Peak current	T_{on}	T_{off}	Dielectric flow rate
1	2.453	1.402	2.435	3.028	2.720
2	2.990	1.675	2.635	2.800	2.565
3	–	5.088	3.095	2.337	2.880
Delta	0.537	3.687	0.660	0.692	0.315
Rank	4	1	3	2	5

level of SR (Ra). For the measurement of SR, smaller is better (S/N ratio) was utilized because the minimum value of SR means the higher value of surface finish.

The rank given in Table 7 shows the influence of parameters on surface roughness. For surface roughness, peak current and T_{on} is the most influencing parameters, whereas the dielectric flow rate has the least significance.

The value of surface roughness is minimum at 1.5° of taper angle, level-1 of I_p, level-1 of T_{on}, level- 3 of T_{off} and level-3 of the dielectric flow rate as shown in Table 8. Therefore, these are the best optimized values for surface roughness.

4.4 Influence of input constraints on MRR

The main effect plot for data means for MRR is shown in Fig. 15. For MRR, larger is better (S/N ratio) was used because the maximum value of MRR means higher the rate of production.
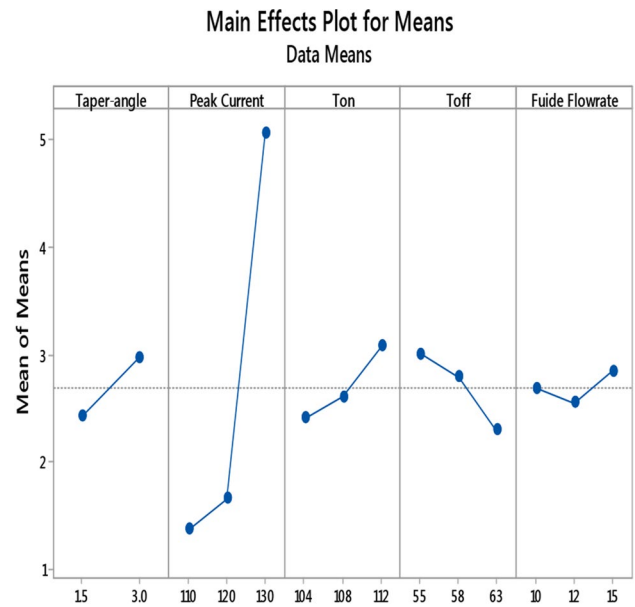
The value of MRR is maximum at 3° of taper angle, level-3 of I_p, level-3 of T_{on}, level-1 of T_{off} and level-3 of the dielectric flow rate as shown in Table 9. Therefore, these are the best optimized values of parameters for MRR. Peak

current and pulse off time has the most influence on MRR whereas the dielectric flow rate has the least significance as shown in Table 10.

5 Conclusions

This paper represents the application of ANFIS model for the prediction of output responses, namely surface roughness and MRR of WEDM parameters. The five input parameters of WEDM, i.e. taper angle, peak current, pulse on time, pulse off time and dielectric flow rate are used as input for ANFIS models for the prediction of output responses. The ANFIS models are compared with a regression model to measure the output performance. From comparison, it is concluded that the ANFIS model performance is better for prediction of surface roughness and MRR than Regression models. The results predicted by ANFIS model have been used to measure the influence of various input parameters on the performance parameters along with the surface view. The developed ANFIS models provide better responses and can be used for more reliable results.

An attempt has also been made to attain minimum and maximum evaluation of surface roughness (SR) and MRR respectively; using multi-parametric optimization namely GRA (grey relational analysis) coupled with Taguchi method. The optimized parameters for the response of SR and MRR in WEDM are: 1.5° of taper angle, 110 amps of peak current, 104 μs of pulse on time, 63 μs of pulse off time and 115 Ltr/min of dielectric flow rate. The attained optimum outcomes had also been examined through a real experiment and established to be satisfactory. For surface roughness, the I_p and T_{on} are the most influencing parameters, whereas for MRR, the I_p and T_{off} are the most influencing parameters. The dielectric flow rate has the least influence on SR as well as on MRR. The experimental results showed the considerable advancement in the process and obtained results will facilitate the WEDM industries to improve the productivity and performance.

Compliance with ethical standards

References

1. Sommer C, Steve Sommer ME (2013) Complete EDM handbook. Reliable EDM, Houston
2. Veiga C (2012) Properties and applications of titanium alloys: a brief review. Rev Adv Mater Sci 32:133–148
3. Kumar S, Mitra B, Dhanabalan S (2018) The state of art: revolutionary 5-axis CNC wire EDM and its recent developments. Int J Manag IT Eng 8:328–353
4. Kumar S, Subramani P (2018) Hybrid optimization of WEDM parameters to predict the influence on surface roughness and cutting speed for Ni-based Inconel 600 wrought superalloy. Int J Mech Prod Eng Res Dev (IJMPERD) 8(2):865–872
5. Anwar S, Nasr MM, Alkahtani M (2017) Predicting surface roughness and exit chipping size in BK7 glass during rotary ultrasonic machining by ANFIS. In: Proceedings of the international conference on industrial engineering and operation management, Rabat, Morocco
6. Miller SF, Shih AJ, Jun Q (2004) Investigation of the spark cycle on material removal rate in wire electrical discharge machining of advanced materials. Int J Mach Tools Manuf 44:391–400
7. Liao YS, Woo JC (1997) The effects of machining settings on the behavior of pulse trains in WEDM process. J Mater Process Technol 71:433–439
8. Mahapatra SS, Patnaik A (2007) Optimization of wire electrical discharge machining (WEDM) process parameters using Taguchi method. Int J Adv Manuf Technol 34:911–925. https://doi.org/10.1007/s00170-006-0672-6
9. Kumar A, Kumar V, Kumar J (2012) Prediction of surface roughness in wire electric discharge machining (WEDM) process based on response surface methodology. Int J Eng Technol 2(4):708–719
10. Manjaiah M, Laubscher RF, Kumar A, Basavarajappa S (2016) Parametric optimization of MRR and surface roughness in wire electro discharge machining (WEDM) of D2 steel using Taguchi-based utility approach. Int J Mech Mater Eng 11:7. https://doi.org/10.1186/s40712-016-0060-4
11. Kumar G, Tiwana JS, Singla A (2016) Optimization of the machining parameters for EDM wire cutting of Tungsten Carbide. In: ICAET, MATEC web of conferences 57:0300. https://doi.org/10.1051/matecconf/20165703006
12. Vijaya Babu T, Soni JS (2017) Optimization of process parameters for surface roughness of Inconel 625 in Wire EDM by using Taguchi and ANOVA method. Int J Curr Eng Technol 7:1127–1131
13. Muniappan A, Thiagarajan C, Somasundaram S (2017) Optimization of kerf width obtained in WEDM of aluminum hybrid composite using Taguchi method. ARPN J Eng Appl Sci 12:382–388
14. Kar S, Das S, Kanti P (2014) Applications of neuro fuzzy systems: a brief review and future outline. Appl Soft Comput J 15:243–259
15. Caydas U, Hascalık A, Ekici S (2009) An adaptive Neuro-fuzzy inference system (ANFIS) model for wire-EDM. Expert Syst Appl 36:6135–6139
16. Hossain SJ, Ahmad N (2012) Adaptive neuro-fuzzy inference system (ANFIS) based surface roughness prediction model for ball end milling operation. J Mech Eng Res 4:112–129
17. Boral S, Chakraborty S (2016) A case-based reasoning approach for non-traditional machining processes selection. Adv Prod Eng Manag 11(4):311–323
18. Sarikaya M, Gullu A (2015) Multi-response optimization of minimum quantity lubrication parameters using Tauchi-based grey relational analysis in turning of difficult-to-cut alloy Haynes 25. J Clean Prod 91:347–357
19. Sarikaya M, Yilmaz V (2016) Optimization and predictive modeling using S/N, RSM, RA and ANNs for micro-electrical discharge drilling of AISI 304 stainless steel. Neural Comput Appl. https://doi.org/10.1007/s00521-016-2775-9
20. Meral G, Sarikaya M, Mia M, Dilipak H, Seker U, Gupta MK (2018) Multi-objective optimization of surface roughness, thrust force and torque produced by novel drill geometries

using Taguchi-based GRA. Int J Adv Manuf Technol. https://doi.org/10.1007/s00170-018-3061-z

21. Chatterjee P, Chakraborty S (2017) A developed meta-model for selection of cotton fabrics using design of experiments and TOPSIS method. J Inst Eng India Ser E 98:79–90

22. Chatterjee P, Mondal S, Boral S, Banerjee A, Chakraborty S (2017) A novel hybrid method for non-traditional machining process selection using factor relationship and multi-attribute border approximation method. Facta Univ Ser Mech Eng 15(3):439–456

23. Jang JR (1993) ANFIS: adaptive-network-based fuzzy inference system. IEEE Trans Syst Man Cybern 23(3):665–685

24. Zalnezhad E, Sarhan AAD, Hamdi M (2013) A fuzzy logic based model to predict surface hardness of thin film TiN coating on aerospace AL_{7075}-T6 alloy. Int J Adv Manuf Technol 68:415. https://doi.org/10.1007/s00170-013-4738-y

25. Abraham A (2005) Adaptation of fuzzy inference system using neural learning. Fuzzy Syst Eng 83:53–83

26. Mohapatraa KD, Satpathya MP, Sahoo SK (2017) Comparison of optimization techniques for MRR and surface roughness in wire EDM process for gear cutting. Int J Ind Eng Comput 8:251–262